Advanced Modeling of Lead Rubber Bearings Under Large Strains

Min Kyu Kim[a] Joaquin Marquez[b], Gilberto Mosqueda[b]

[a]*Structural and Seismic Safety Research Team, Korea Atomic Energy Research Institute, 989-111 Daedeok-daero, Youseong, Daejeon, 34057*
[b]*Department of Structural Engineering, University of California - San Diego, USA*

**Corresponding author:minkyu@kaeri.re.kr*

1. Introduction

In an effort to develop reliable bearing models that are able to capture the behavioral characteristics of lead-rubber bearings under large amplitude cyclic displacements, elastomeric bearing models available in OpenSees are first reviewed. While certain models capture key characteristics, a model demonstrating the capacity to capture the actual complex responses of LRBs has not yet been implemented. Characteristics of particular interest include the strength reduction in the bearing due to the heating of the lead core as well as hardening at high strains. To remedy extant deficiencies, it will be demonstrated that calibrating a combination of parallel models can be an effective approach to achieve adequate results that reflects actual bearing behavior. In this chapter, a summary of each element will be discussed, as well as the combinations of the models that were utilized to capture behavior demonstrated in experimental data for large bearings. In order to evaluate the responses of the different models under earthquake excitation, a SDOF 1D model analysis is presented using these more complex models.

2. LeadRubberX Element

In order to capture both the strength reduction in the bearing due to the heating of the lead and the hardening due to high strains, two models were combined in parallel. The OpenSees model used to capture the lead heating effect in the parallel model is LeadRubberX (LRX). This coupled bi-directional model's hysteresis is isotropic in nature due to the degradation of the hysteresis (i.e. the characteristic strength of the lead). The force-displacement relation of LRX model is shown in Figure 1.

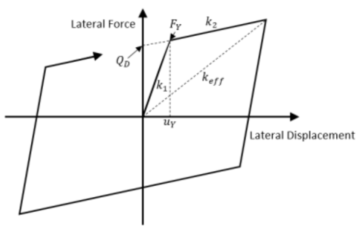

Figure 1. LRX Hysteresis

3. Bouc-wen (Hardening) Element

The second element in the parallel system that can capture the hardening of the LRB at high strains is the Bouc-Wen Bearing, implemented in OpenSees by Schellenberg.

The advantage of combining both models in parallel is that the various nonlinearities that are seen in LRBs can be captured. In Figure 2, both elements are working in parallel to capture the hardening effect and strength degradation. The hardening element only accounts for the nonlinearities due to the high strains as shown in Figure 2.

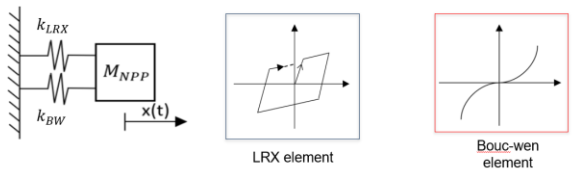

Figure 2. Parallel System (Heating-Hardening Bearing).

$$\begin{Bmatrix} F_x \\ F_y \end{Bmatrix} = K_2 \cdot \begin{Bmatrix} U_x \\ U_y \end{Bmatrix} + (\sigma_{YL}(T_L)A_L) \cdot \begin{Bmatrix} Z_x \\ Z_y \end{Bmatrix} + K_3 \cdot \mathrm{sgn}\begin{Bmatrix} U_x \\ U_y \end{Bmatrix} \cdot \begin{vmatrix} U_x^{\mu} \\ U_y^{\mu} \end{vmatrix} \qquad (4-1)$$

4. Calibration of Models

In order to calibrate model parameters based on the available experimental data that already performed by Kim et al [1], the initial design values from the manufacture were first set as preliminary parameters. The initial stiffness, post-yield stiffness and characteristic strength is calibrated using test data at moderate levels of shear strains, e.g. 100%-300% shear strains. For tests at higher strains in the range of 300%-500% shear strain, calibration for K_3 and μ were conducted. Different types of optimization schemes were considered such as Matlab functions Fminsearch (the Nelder-Mead simplex algorithm), Fmincon (Constrained Nonlinear Optimization algorithms), Genetic Algorithm (GA), and Particle Swarm Optimization (PSO). Fminsearch and GA, for this purpose, deemed the best methods to finding the set of parameters that minimized the defined error. The error measure that was used was the Normalized Root Mean-Squared Error (NRMSE), as shown in Eq. 1.

$$NRMSE\,(\%) = \frac{\sqrt{\frac{1}{N}\sum_{i=1}^{N}(F_{exp} - F_{num})}}{(F_{max} - F_{min})} \cdot 100\% \quad (1)$$

This calibration was applied for 1-D and compared with different configurations, to commence, the LRX itself and LRX-Hardening parallel system was utilized, for short (H-H model) (i.e. including heating of the lead and hardening). As shown in Figures 3 and 4, the hardening element is able to capture the hardening portion of the experimental data and therefore reducing the NRMSE.

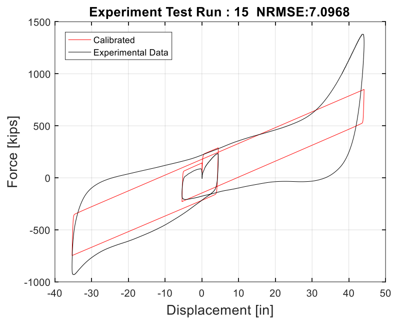

Figure 3. LRX Calibration (500% Shear Strain Test).

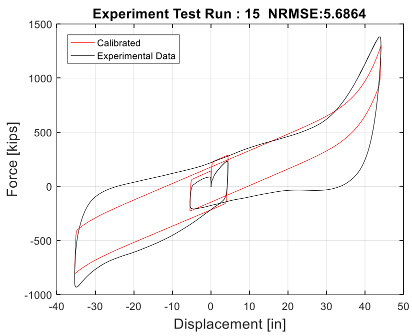

Figure 오류! 지정한 스타일은 사용되지 않습니다.. LRX-BW Calibration (500% Shear Strain Test).

5. HDR Element

Although improvements were made by the parallel system, there are evident shortcomings of the model. As can be seen in Figure 4, the H-H model poorly estimates the resisting force at the displacement reversals during unloading. To better capture this behavior, the introduction of the HDR element to the existing model is examined. The same concept is maintained using the elements in parallel as previously mentioned. The combined model, for short, is named as H-H-HDR model.

As mentioned by Grant [2], scragging depends on the previous maximum strains while Mullins' effect decreases in strength as it is being cycled and can occur repetitively, as demonstrated in Figure 5. Two analyses will be conducted one with damage parameters and one without. The evolution of the damage parameters can be seen in Figure 5, where D_s is the scragging damage parameter and D_M, is the damage parameter for Mullins' effect. With the experimental data, it was observed that Mullins' effect was negligible and therefore it was not used for this study.

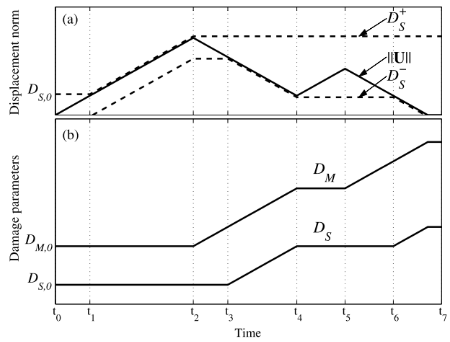

Figure 5. Scragging parameters evolution due to displacement norm.

With bounding of the parameters specified, the model can be calibrated by using a multi-objective optimization for all tests. Note that these 1-D calibrations may not be representative of the bearing in 2-D due to the fact that the hysteresis component has a dependency on the velocity vector direction which can result in unrealistic 2-D results after optimizing for 1-D. The calibrated H-H-HDR model for test is shown in Figure 6, this combination of models is able to capture the hardening and the 'Bauschinger' effect at the reversals.

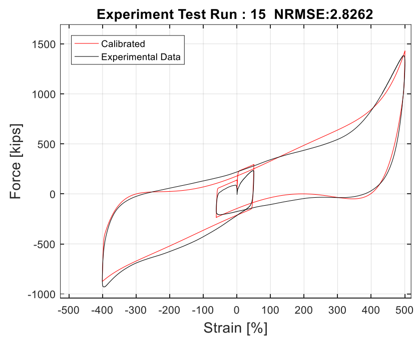

Figure 6. H-H-HDR calibration (500%) shear strain test.

6. SDOF 1D Analysis

A SDOF 1-D analysis was conducted to observe the hysteresis of the different models under earthquake excitation and the displacement demands that result for various ground motions. In this SDOF system, no actual moat wall pounding is considered but the velocity is recorded at a given displacement that could be representative of a moat wall clearance. The reason for considering a fictious moat wall clearances is to evaluate the differences between the models and the effects the nonlinear H-H-HDR model may have on impact velocity. Using the calibrated models, a SDOF system was analyzed under a set of 20 different ground motions. Pseudo acceleration response spectra for the set of 20 dispersion are shown in Figure 7.

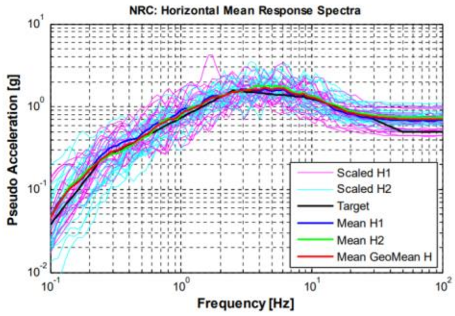

Figure 7. Pseudo acceleration response spectra for the set of 20 dispersion -appropriate motions selected to match 5% damped USNRC RG1.60 target spectrum with a PGA = 0.3g in an avg. sense over the frequency range from 0.25Hz-20Hz.

H-H-HDR was set to the calibrated parameters but allowed for heating and hardening to occur in the parallel system. In Figure 4-12, it can be seen that for the 12th ground motion and for all other cases the H-H-HDR bearing has much smaller displacements compared to the heating case, indicating the importance of including hardening. Also, the heating case has much larger displacements compared to the Bilinear model with no heating considered. The damage case shows that scragging has taken effect with the restoring force about -700 kips at -300% strain while in the positive 300% strain it is at slightly above 600 kips. This initial hardening due to scragging reduced the displacements for the HHHDR compared to no damage HHHDR with a strain reduction of 20%.

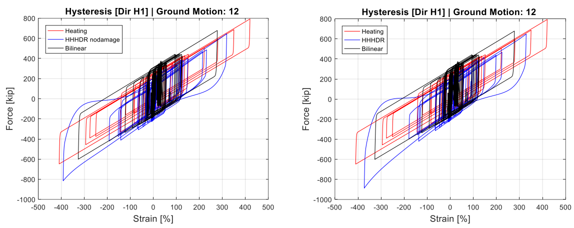

Figure 8. Ground Motion 12 Hystersis Comparison | Left: Damage included in HHHDR | Right: No damage in HHDR.

7. Maximum Displacement Comparison

To present of summary of the results from all the analysis conducted, the maximum displacements are shown in Figure 9 for the three different systems. The displacements with damage are shown for H-H-HDR due to the fact that the displacements were not significantly different from the no damage case. In the next section, it will be seen that although the displacements were the same, the impact velocities changed significantly. The displacements for the H-H-HDR system for all cases were less than the heating case. For ground motions 7, 8, 11, and 15 the displacements were further reduced to less than the bilinear system. This shows that although heating occurred for the H-H-HDR system, the hardening and 'Bauschinger' effect was able to counteract the heating effects and further reduce the displacements compared to the bilinear system. The average displacement for LRX model, H-H-HDR with damage, and Bilinear were 36.1, 30.4 and 28.0 inches, respectively.

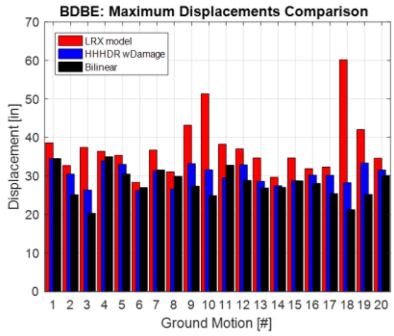

Figure 9. Maximum displacement comparison for each GM.

8. Moat Wall Impact Velocity

For this 1D SDOF system, a fictious wall clearance was implemented at different displacements to observe potential effects at first impact. The purpose of these analysis was to observe the effects different models would have on the impact velocity or severity of impact by considering the moat wall a different distance. Due to the fact that the first impact would affect the second impact and no real moat wall was implemented, for this analysis, only the first impact velocity was analyzed. In Figure 10, it can be seen that for each model as the CS is increased the impact velocity decreases. The heating case has the higher velocity impact for each clearance to stop due to the loss of strength and energy dissipation is reduced as it is being cycled. The bilinear case resulted in the lowest velocity, as expected. The H-H-HDR with damage was able to further reduce the speed at impact compared to H-H-HDR without damage. This is due to the fact that the stiffening effect is higher for the HHHDR damage model. Although the model reduces the stiffness after the maximum displacement magnitude is reached from the previous cycle, it is able to reduce the speed of the high demand portion of the ground motion, where impact will more likely occur. These results indicate the sensitivity of results for analysis of base isolated building considering various bearing models.

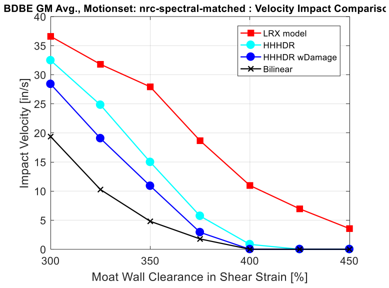

Figure 10. Impact velocity comparison for each GM.

8. Conclusion

The different bearing models available in OpenSees are examined with models containing key characteristic behavior combined to capture experimentally observed bearing behavior. The resulting parallel H-H-HDR model calibrated and shown to provide a good match to the experimental data. The model is a combination of the LeadRubberX (LRX), Bouc-Wen (hardening), and the HDR elements from OpenSees. The models are able to capture the strength degradation due to heating of the lead, hardening at high strains, and the 'Baushinger effect' that are observed in physical LRBs. With calibration complete for the H-H-HDR model, a SDOF 1D analysis is conducted to examine the effects of capturing the reversals and the hardening effect have on the system. In this study it was found that the first impact velocity at different Clearance to Stops (CS), resulted in the H-H-HDR model to be bounded by the degrading heating case and the non-degrading strength case. It was also observed that when including the ability for scragging to occur will result in reduced impact speeds compared to the case with scragging damage parameters not accounted for. This is important since scragging effects recover within a year and the likelihood of a BDBE earthquake to occur in more than 1 year from a prior BDBE motion or after installation is high. These analyses were conducted for 1D motions and A 2D model with the capabilities of being able to account for hardening and the 'Baushinger' effect will be implemented in a future chapter in order to obtain more details of the response of the H-H-HDR model.

ACKNOWLEDGEMENT

This work was supported by Nuclear Research & Development Program of the National Research Foundation (NRF) grant funded by the Korean government (MEST).

Reference

[1] M. K. Kim, J. H. Kim, Performance characteristics of seismic isolation devices for nuclear power plants according to real and small scale model test, Transactions, SMiRT-24, BEXCO, Busan, Korea - August 20-25, 2017

[2] D. Grant, "Bidirectional Modelling of High-Damping Rubber Bearings," 2004.